Purinergic Signalling (2006) 2:343–350
DOI 10.1007/s11302-006-9000-8

ORIGINAL ARTICLE

Ecto-5′-nucleotidase: Structure function relationships

Norbert Sträter

Received: 7 October 2005 / Accepted: 20 December 2005 / Published online: 16 May 2006

Abstract Ecto-5′-nucleotidase (ecto-5′-NT) is attached via a GPI anchor to the extracellular membrane, where it hydrolyses AMP to adenosine and phosphate. Related 5′-nucleotidases exist in bacteria, where they are exported into the periplasmic space. X-ray structures of the 5′-nucleotidase from *E. coli* showed that the enzyme consists of two domains. The N-terminal domain coordinates two catalytic divalent metal ions, whereas the C-terminal domain provides the substrate specificity pocket for the nucleotides. Thus, the substrate binds at the interface of the two domains. Here, the currently available structural information on ecto-5′-NT is reviewed in relation to the catalytic properties and enzyme function.

Key words CD73 · ecto-enzymes · nucleotidase

Abbreviations
5′-NT 5′-nucleotidase

Biological function

5′-nucleotidases (5′-NT, E.C. 3.1.3.5) catalyse the hydrolysis of the phosphoric ester bond of 5′-ribonucleotides to the corresponding ribonucleoside and phosphate. These enzymes have been found in bacteria, animals and plants and they display significant differences in the range of substrates hydrolysed. In the animal enzymes one has to distinguish between the cytosolic and the extracellular, surface-located ecto-enzymes, which are structurally unrelated [1]. Cytosolic 5′-NT controls the intracellular levels of nucleoside 5′-monophosphates.

On the basis of the primary sequence homology it became clear that ecto-5′-NT is related to the bacterial 5′-nucleotidases. Characteristic sequence motifs showed furthermore, that the enzyme belongs to a superfamily of metallophosphoesterases with a dinuclear metal center [2].

The main function of 5′-NT is the hydrolysis of AMP to adenosine. It is thus part of the cascade (together with ecto-ATPases) to terminate the action of nucleotides such as ATP as extracellular signalling molecules acting on P2X and P2Y receptors [3]. On the other hand, the enzyme generates adenosine, which acts on P1 receptors. There is evidence for a coordinated induction and repression of ecto-5′-NT and the A2a adenosine receptor in human B-cell lines [4]. The enzyme is also important for the recycling of extracellular nucleotides, which are converted to nucleosides by 5′-NT and internalized through specific nucleoside transporters. Purinergic receptor signalling is involved in very diverse biological processes including neurotransmission, platelet aggregation, modulation of the immune response, smooth muscle contraction as well as the control of cell proliferation, differentiation and apoptosis [5, 6]. Specific inhibitors against the hydrolytic enzymes including 5′-NT and synthetic ligands acting as agonists or antagonists of the purinergic receptors have therapeutic potential. Like other surface-located enzymes, ecto-5′-NT, also known as CD73, has been implicated in non-enzymatic functions such as T-cell activation and cell–cell adhesion [7, 8].

N. Sträter (✉)
Center for Biotechnology and Biomedicine,
University of Leipzig,
Deutscher Platz 5, 04103 Leipzig, Germany
e-mail: strater@bbz.uni-leipzig.de

Catalytic properties

5′-NT shows no activity towards nucleoside 2′- and 3′-monophosphates ([5] and references therein). The hydrolysis of 5′-AMP is stereoselective, since the L-enantiomer is no substrate [9]. The K_m values for 5′-AMP as the best substrate are in the low micromolar range. ADP and ATP are competitive inhibitors, with inhibition constants also in the low micromolar range. This indicates that they bind similarly to the active site but cannot be hydrolyzed. This is in contrast to *E. coli* 5′-NT which hydrolyses AMP, ADP, and ATP and other 5′-ribo- and 5′-deoxyribonucleotides [10, 11]. The bacterial enzyme also hydrolyzes the artificial substrate *p*-nitrophenyl phosphate, which is not a substrate for ecto-5′-NT [5]. On the other hand, purified 5′-NT from the electric ray hydrolyses UDP-glucose as does *E.coli* 5′-NT [12]. The bacterial as well as the vertebrate enzymes show no product inhibition by phosphate, in contrast to the related purple acid phosphatases and Ser/Thr protein phosphatases. The pH optimum is between 7 and 8. A comprehensive reference to the molecular and kinetic characterisation of 5′-NT until 1992 is found in [5].

Structural properties

Determination of the primary structures of ecto-5′-NT from human placenta [13], rat liver [14] and the electric ray fish [12] showed that the mature enzyme consists of 548 amino acids with a calculated molecular mass of 61 kDa. A stretch of ~25 hydrophobic residues at the C-terminus is replaced by a glycosyl phosphatidylinositol (GPI) anchor, by which the mature protein is attached to the cell membrane via the C-terminal serine residue linked to a complex oligoglycan and a sphingolipidinositol group [15]. No protein segments are embedded within the membrane [16]. Soluble forms of the enzyme exist [17–19], which are derived from the membrane-bound form by hydrolysis of the GPI anchor by phosphatidylinositol-specific phospholipase [18, 20] or by proteolytic cleavage [19]. Chicken gizzard 5′-NT also binds with high affinity to the laminin/nitogen complex [21].

The mammalian enzymes display a sequence identity of slightly more than 20% to the bacterial enzymes, indicating a common ancestry and similar structures. On the basis of short sequence motifs it became clear that ecto-5′-NT belongs to a large superfamily of distantly related metallophosphoesterases acting on diverse substrates such as Ser/Thr phosphoproteins, various nucleotides, sphingomyelin, as well as RNA and DNA [2]. The first crystal structures of these metallophosphatases, a plant purple acid phosphatase [22] and mammalian Ser/Thr protein phosphatases [23–26] showed a common core fold consisting of four layers with two mixed sandwiched β-sheets flanked by α-helices (layers αββα). Two metal ions are present in the catalytic center.

For ecto-5′-NT isolated from three different sources Fini et al. [27] determined a metal content of two zinc ions per dimer, indicating that at least one of the two metal binding sites is occupied by zinc. For the monomeric *E. coli* 5′-NT two bound zinc ions have been determined [28]. This finding is in contrast to earlier studies where a zinc/protein ratio of 0.7 has been found [29]. Possibly, part of the metal has been dissociated due to the low binding affinity of one metal site. Different metal binding affinity of the dimetal center is supported by kinetic and mutational as well as crystallographic data [28, 30]. Analysis of metal activation of variants with mutated metal ligands indicates that M2 has a lower affinity for Zn^{2+} and that it is the site of Co^{2+}-activation [28]. M1 has a lower affinity for Mn^{2+} compared to M2, as shown by the occupancy of the metal binding sites in the crystal. Bovine and rat ecto-5′-NT display the largest catalytic activity by activation with cobalt ions [29, 31], similar to the *E. coli* enzyme [10, 28, 32], whereas electric ray 5′-NT is maximally activated by Mg^{2+} and Ca^{2+} [33].

Ecto-5′-NT forms homodimers [34, 35], which are not linked by cystine bridges [36]. In the enzyme from bull seminal plasma, the eight cysteines are all involved in intramolecular disulfide bridges of the following pairs: Cys51–Cys57, Cys353–Cys358, Cys365–Cys387 and Cys476–Cys479 [37]. For this enzyme the *N*-glycosylation of Asn53, Asn311, Asn333 by high-mannose saccharide chains and of Asn403 by a mixture of high mannose and complex type glycans amounted to ~6 kDa molecular weight of the 65.6 kDa protein. The glycosylation is highly heterogenous, especially at Asn403 and the resulting isoforms differ significantly in substrate specificity and catalytic activity [19].

3D structure

A crystal structure is available for *E. coli* 5′-NT (Fig. 1) [38]. The enzyme consists of two domains: The N-terminal domain (residues 25–342) binds the two metal ions and contains an Asp–His dyad, which are important for the catalytic activity. This domain is related

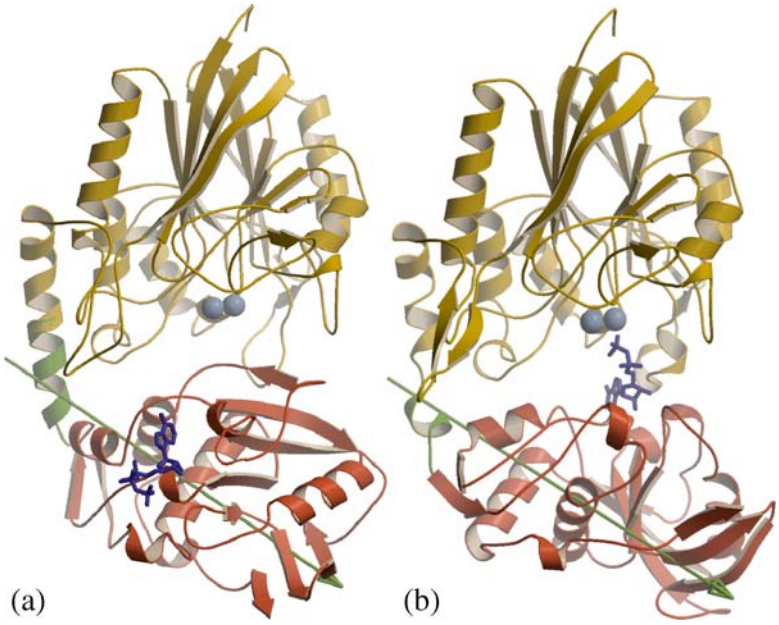

Fig. 1 Fold of *E. coli* 5′-NT. (a) Open form in complex with ATP (b) Closed form with the inhibitor α,β-methylene-ADP bound to the active site. The substrate and inhibitor are shown in *blue*. ATP is bound to the same binding site of the C-terminal domain in the *open form* as the inhibitor in the *closed form*. The substrate rotates with the C-terminal domain into the proximity of the dimetal center (shown in *light blue*) by a 96°-domain rotation around the axis depicted in *green*. The N-terminal domain is coloured in *yellow*, the C-terminal domain in *red* and the bending residues of the hinge region in *green*.

to other known enzyme structures of the calcineurin superfamily of dimetal phosphoesterases and it has the characteristic four-layered fold described above. The C-terminal domain (residues 362–550) has a unique structure, which has so far not been found in other protein structures. This domain provides the binding site for the adenosine moiety of the substrate. Thus, the active site is located between the two domains. A long α-helix (residues 343–361) connects the two domains.

In the crystal structures, the protein has been characterised in two different conformations, which differ in the relative orientation of the two domains [39]. The domain movement can be described as a rotation of the C-terminal domain around the axis shown in Fig. 1, which passes through the center of the C-terminal domain. A rotation of up to 96° is necessary for the change between the inactive open and the active closed conformation. The domain rotation is necessary for the catalytic action of the enzyme, presumably to allow for substrate binding and product release [40, 41].

A model for the mammalian ecto-nucleotidases

A sequence alignment of *E. coli* 5′-NT and the mammalian ecto-enzymes shows that both domains are conserved and a homology model can be built for ecto-5′-NT (Figs. 2 and 3). The alignment shown in Fig. 2 is manually edited based on an automated sequence alignment and based on information from the generated models in order to fulfill structural constraints such as the possibility to form the known cystine bridges [37] and the necessary insertions and deletions.

In this model the loop from residue 319 to 337 in the *E. coli* enzyme, stabilized by two interacting β-strands, is missing in ecto-5′-NT (L1 in Fig. 3). This loop is pointing away from the enzyme and has few interactions with the protein. Its function is unknown. The nearby loop around residue 50 is longer in the mammalian enzyme (L2). It is stabilized by a cystine bridge (51–57) and carries a glycosylation on Asn53. On the other side of the protein, three loops are predicted to differ significantly between the mammalian and bacterial nucleotidases. The loop near residue 146 in *E. coli* (L3) is longer in the mammalian enzymes whereas the short helix at residue 183 in *E. coli* 5′-NT is missing (L4). In the C-terminal domain two insertions are predicted to be present in ecto-5′-NT: At residue 482 (L5) and 398 (L6) of the bacterial sequence. The loop around residue 228 in *E.coli* 5′-NT is significantly shorter in ecto-5′-NT (L7). Further smaller insertions and deletions are present in the model.

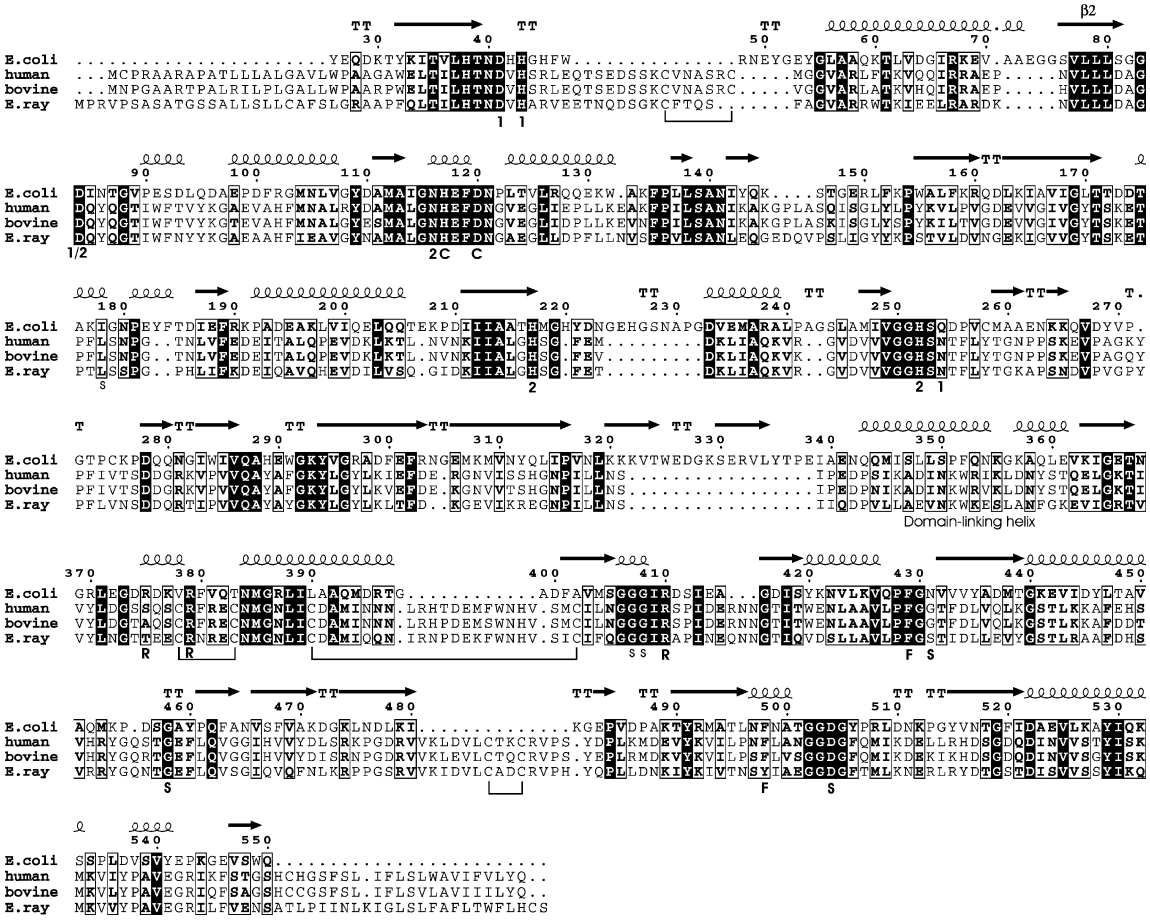

Fig. 2 Sequence alignment of *E. coli*, bovine, human and electric ray 5′-nucleotidases. The secondary structure and the residue numbering shown above the alignment are from the *E. coli* structure. Functionally important residues are marked below the alignment with the following labels: ‘1’ and ‘2’ mark ligands to metal ions 1 and 2, respectively; the catalytic Asp–His dyad is labeled ‘C’; ‘R’ marks the three arginine side chains in the active site of the *E. coli* enzyme; ‘F’ are the phenylalanines that bind the adenine moiety; residues that interact with the substrate by hydrogen bonding are marked with a capital ‘S’ whereas residues involved in non-polar interactions are indicated by a lower-case ‘s’. *Cystine bridges* of the bovine enzyme are marked by *lines* connecting the cysteines.

The mammalian enzymes form dimers, whereas the bacterial enzymes are monomers. It is not possible to predict the interaction site between the monomers with confidence, however, it is unlikely that the left side of the monomer as depicted in Fig. 3 forms the dimer interface since it carries several glycosylation sites. It is more likely that the other side of the protein near loops L3 and L4 is part of the dimer interface. If a domain rotation is also part of the catalytic cycle of the mammalian enzymes, it might be speculated that the two monomers interact only with the larger N-terminal domains and not at the smaller C-terminal domain, which rotates around its center in the *E. coli* enzyme.

It is at present not clear how the glycosylation sites could modulate the enzyme activity [19], since they are relatively far away from the active site. Asn-333 is located close to the hinge region and its glycosylation might influence a domain movement in ecto-5′-NT (Fig. 3). An influence of the different charge of the heterogenously sialylated glycans by long-range electrostatic interactions is also possible [19].

Dimetal site

The two metal ions in the active site of *E. coli* 5′-NT are 3.3 to 3.5 Å apart and are bridged monodentately by an aspartate side chain and by a water molecule (Fig. 4). Metal ion 1 is further ligated by an aspartate, a glutamine and a histidine residue. A water molecule completes the octahedral coordination sphere if Mn^{2+} is bound. Metal ion 2 is coordinated by two histidines and an asparagine side chain as well as by a water molecule, which is replaced by the phosphate group of the substrate in the Michaelis complex. In the dizinc enzyme both metal ions are five-coordinated since the

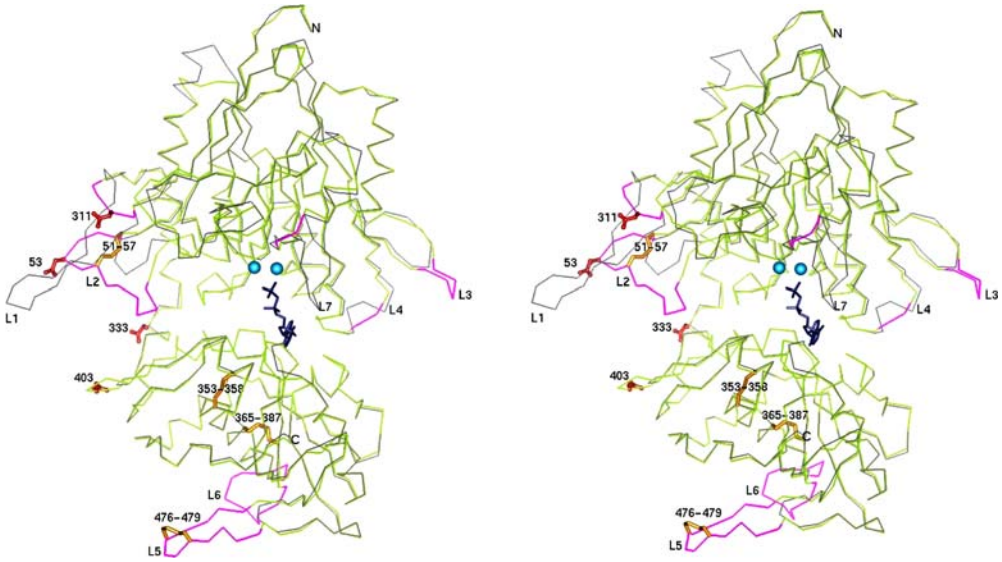

Fig. 3 Superposition of the C_α traces of the experimental X-ray structure of *E. coli* 5′-NT (protein C of PDB ID 1HPU; *grey*) and the homology model for human 5′-NT. Larger insertions and deletions of the ecto-5′-NT are coloured in *magenta* and labeled L1 to L7. The closed conformation of *E. coli* 5′-NT (protein C of PDB ID 1HPU) has been used as template for the homology modelling according to the sequence alignment listed in Fig. 2). The exact loop conformations of longer insertions (L2, L3, L5 and L6) in ecto-5′-NT cannot be modeled with confidence. The experimentally determined disulfide bridges of bovine 5′-NT are shown in *yellow* and the glycosylated asparagines are shown in *red*. Depicted in *dark blue* is the substrate analogue inhibitor α,β-methylene-ADP.

terminal water ligands are missing [38]. The metal ligands are all conserved in ecto-5′-NT with the exception of M1-ligand Gln254 which corresponds to Asn245 in ecto-5′-NT. It appears unlikely that the shorter side chain supports metal coordination of Asn245, but the Asn245 carboxamide group may bind a water molecule which is coordinated to M1. This situation is similar in the Ser/Thr protein phosphatases, where also a water molecule is coordinated to M1 in place of the Gln of *E. coli* 5′-NT.

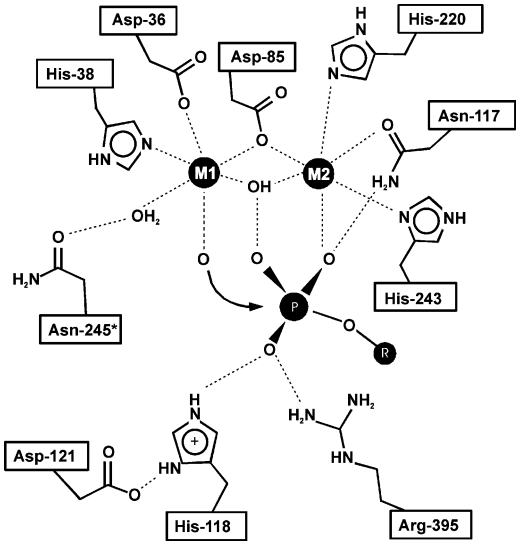

Fig. 4 Scheme of the dimetal center and proposed structure of the Michaelis complex for 5′-NT catalysis. The binding mode of the substrates terminal phosphate group is supported by the binding mode of the inhibitor α,β-methylene-ADP. Residue labels refer to human 5′-NT. All residues except for Asn245 are conserved in the *E. coli* enzyme. Therefore the coordination of Asn245 *via* a water molecule to metal ion 1 is hypothetical. In the bacterial enzyme Asn245 is replaced by a glutamine, which is directly coordinated to the metal ion.

Substrate binding site

Structures of *E. coli* 5′-NT in complex with the substrate analogue inhibitor α,β-methylene-ADP revealed the characteristics of the substrate binding pocket of the C-terminal domain (Fig. 5). A central feature is the hydrophobic stacking interaction of the adenine moiety, which is sandwiched between two phenylalanine side chains. The N1 nitrogen of the adenine ring is recognized by the carboxamide group of Asn431. The ribose group of the nucleotide is bound by Asp504, the backbone oxygen of Gly458 and Arg410. Two further arginines are in contact to the α- and β-phosphate groups of the substrate.

Of these residues, the two phenylalanines are conserved in the ecto-enzymes or in electric ray 5′-NT are replaced by a tyrosine, which should also support the stacking interaction. Asn431 is replaced by a glycine residue. There is no other side chain nearby in the model which could replace the asparagine. Most

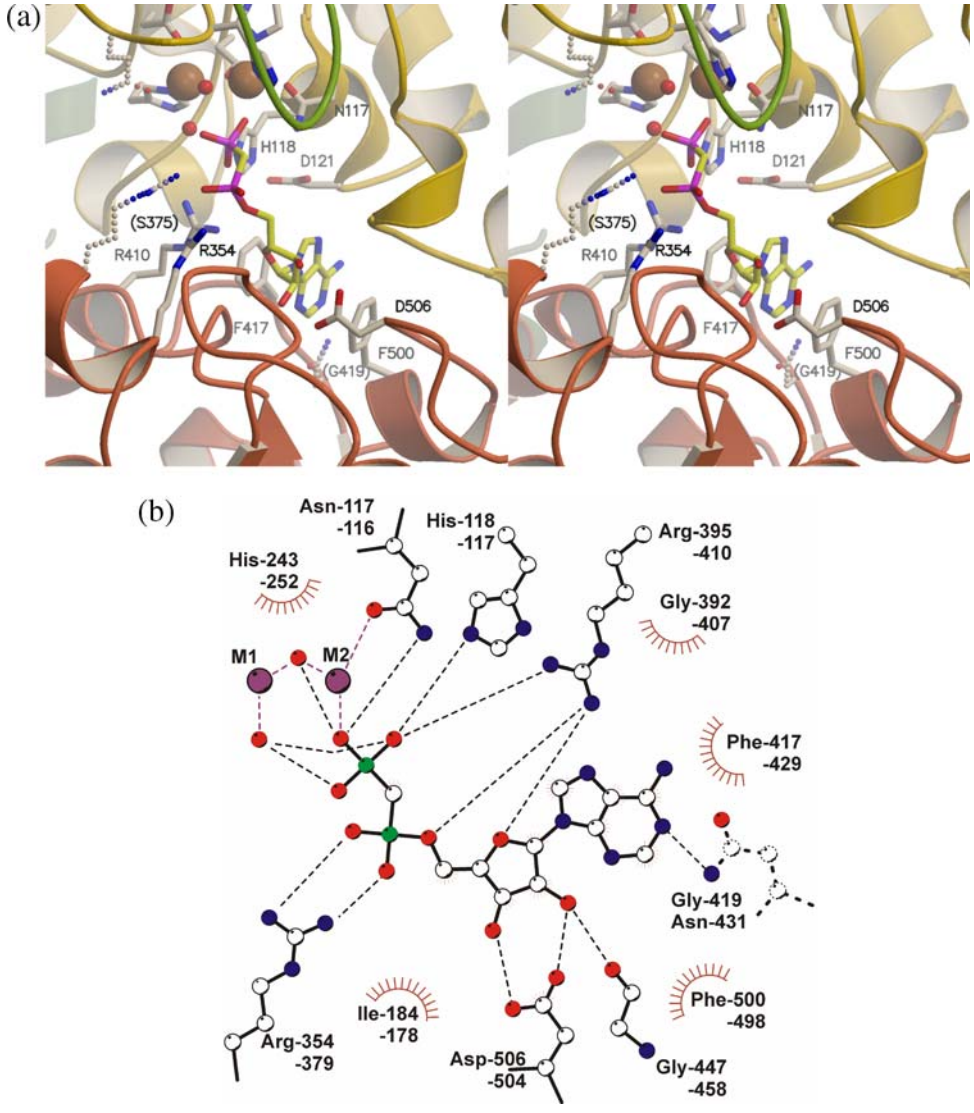

Fig. 5 Binding mode of the substrate analogue inhibitor α,β-methylene-ADP. (a) Stereo view of the active site. The residues which are not conserved in ecto-5′-NT are depicted in *broken lines*. The labels refer to the human enzyme. The loop shown in *green* is predicted to be shorter in the ecto-enzymes. It is labeled L7 in Fig. 3. The colouring of the protein domains is the same as in Fig. 1. (b) Scheme of the interaction between the protein and the inhibitor. The *upper label* for each residue refers to human 5′-NT and the *bottom label* to *E. coli* 5′-NT. All residues are conserved with the exception of Asn-431 of *E. coli* (shown in *broken lines*), which is a glycine in the mammalian enzymes.

likely, a water molecule interacts with N1 of the adenine ring. The aspartate residue bound to the hydroxyl groups of the ribose is conserved, as well as two of the three arginines. Arg375 of the *E. coli* enzyme is replaced by a serine. Thus, from the differences in the substrate binding site it is not obvious how the stronger substrate specificity of the mammalian enzymes towards AMP (vs. ADP and ATP) is achieved. Possibly, a control of the domain rotation and thus the distance between the adenosine binding site of the C-terminal domain and the catalytic metal center of the N-terminal domain influences the activity towards adenine nucleotides that differ in the distance between the adenine moiety and the terminal phosphate group.

Catalytic mechanism

A complex structure with the inhibitor α,β-methylene-ADP provides a model for the substrate binding mode (Figs. 4 and 5) [30]. One oxygen atom of the terminal phosphate group is coordinated to the site 2 metal ion. In addition, the catalytic histidine and an arginine bind and polarize the phosphate group for attack of the nucleophile. The nucleophilic water is supposed to

be the terminal water coordinated to the site 1 metal ion [30]. This water molecule is in a perfect position for an in-line attack on the phosphorus atom. It is located at a distance of 3.2 Å and the angle between this water, the phosphorus atom, and the leaving group is 155°. However, the metal bridging water ligand is also a possible candidate for the nucleophile. The two metal ions, the arginine and the catalytic histidine stabilize the transition state. No protein residue is positioned to protonate the leaving group. Therefore, a water molecule might provide a proton for the leaving group.

This model for the mechanism describes the chemical steps to hydrolyze phosphate ester or anhydride bonds. As mentioned before, in *E. coli* 5′-NT a domain rotation is necessary for catalytic activity, presumably for substrate binding and product release. It is unclear if a domain rotation is also part of the catalytic cycle for the ecto-enzymes. The homology model indicates that the active site might be somewhat more easily accessible in ecto-5′-NT due to the shorter loop L7.

Conclusions

The catalytic domain of extracellular 5′-nucleotidases in bacteria as well as mammals belongs to a large superfamily of dinuclear metallophosphoesterases, which hydrolyse very different substrates, including phosphoproteins, nucleotides and nucleic acids. In 5′-NT, the substrate specificity is provided by the binding pocket for the nucleoside in the unique C-terminal domain. Based on several crystal structures of *E. coli* 5′-NT, the tertiary structure, substrate-binding mode and catalytic mechanism have been characterised. In the absence of crystallographic data of the ecto-5′-NTs, a model can be built for the mammalian 5′-NTs based on the homology of both domains. Open questions are if a domain rotation is also part of the catalytic cycle of ecto-5′-NT and the structure of the dimeric enzyme. Although some differences in the active site structures of ecto-5′-NT and *E. coli* 5′-NT can be derived from the model, further experiments are necessary to verify the homology model and to relate the structural differences to the variation in substrate specificity.

References

1. Hunsucker SA, Mitchell BS, Spychala J (2005) The 5′-nucleotidases as regulators of nucleotide and drug metabolism. Pharmacol Ther 107:1–30
2. Koonin EV (1994) Conserved sequence pattern in a wide variety of phosphoesterases. Protein Sci 3:356–8
3. Zimmermann H (2000) Extracellular metabolism of ATP and other nucleotides. Naunyn–Schmiedeberg's Arch Pharmacol 362:299–309
4. Napieralski R, Kempkes B, Gutensohn W (2003) Evidence for coordinated induction and repression of ecto-5′-nucleotidase (CD73) and the A2a adenosine receptor in a human B cell line. Biol Chem Hoppe–Seyler 384:483–487
5. Zimmermann H (1992) 5′-nucleotidase: molecular structure and functional aspects. Biochem J 285:345–365
6. Goding JW, Grobben B, Slegers H (2003) Physiological and pathophysiological functions of the ecto-nucleotide pyrophosphatase/phosphodiesterase family. Biochim Biophys Acta 1638:1–19
7. Resta R, Yamashita Y, Thompson LF (1998) Ecto-enzyme and signaling functions of lymphocyte CD73. Immunol Rev 161:95–109
8. Spychala J (2000) Tumor-promoting functions of adenosine. Pharmacol Ther 87:161–173
9. Cusack N, Pearson JD, Gordon JL (1983) Stereoselectivity of ectonucleotidases on vascular endothelial cells. Biochem J 214:975–981
10. Neu HC (1967) The 5′-nucleotidase of *Escherichia coli*. I. Purification and properties. J Biol Chem 242:3896–904
11. Glaser L, Melo A, Paul R (1967) Uridine diphosphate sugar hydrolase. Purification of enzyme and protein inhibitor. J Biol Chem 242:1944–1954
12. Volknandt W, Vogel M, Pevsner J et al (1991) 5′-nucleotidase from the electric ray electric lobe. Primary structure and relation to mammalian and procaryotic enzymes. Eur J Biochem 202:855–861
13. Misumi Y, Ogata S, Ohkubo K et al (1990) Primary structure of human placental 5′-nucleotidase and identification of the glycolipid anchor in the mature form. Eur J Biochem 191:563–569
14. Misumi Y, Ogata S, Hirose S, Ikehara Y (1990) Primary structure of rat liver 5′-nucleotidase deduced from the cDNA. Presence of the COOH-terminal hydrophobic domain for possible post-translational modification by glycophospholipid. J Biol Chem 265:2178–2183
15. Ogata S, Hayashi Y, Misumi Y, Ikehara Y (1990) Membrane-anchoring domain of rat liver 5′-nucleotidase: identification of the COOH-terminal serine-523 covalently attached with a glycolipid. Biochemistry 29:7923–7927
16. Fini C, Bertoli E, Albertini G et al (1994) Reconstitution of 5′-nucleotidase of bull seminal plasma in spin-labelled liposomes. J Membr Biol 142:137–144
17. Wortmann RL, Veum JA, Rachow JW (1991) Synovial fluid 5′-nucleotidase activity. Relationship to other purine catabolic enzymes and to arthropathies associated with calcium crystal deposition. Arthritis Rheum 34:1014–1120
18. Klemens MR, Sherman WR, Holmberg NJ et al (1990) Characterization of soluble vs membrane-bound human placental 5′-nucleotidase. Biochem Biophys Res Commun 172:1371–1377
19. Fini C, Talamo F, Cherri S et al (2003) Biochemical and mass spectrometric characterization of soluble ecto-5′-nucleotidase from bull seminal plasma. Biochem J 372:443–451
20. Vogel M, Kowalewski H, Zimmermann H et al (1992) Soluble low-K_m 5′-nucleotidase from electric-ray (*Torpedo marmorata*) electric organ and bovine cerebral cortex is derived from the glycosyl-phoshatidylinositol-anchored ectoenzyme by phospholipase C cleavage. Biochem J 284:621–624
21. Stochaj U, Mannherz HG (1992) Chicken gizzard 5′-nucleotidase functions as a binding protein for the laminin/nidogen complex. Eur J Cell Biol 59:364–372

22. Sträter N, Klabunde T, Tucker P et al (1995) Crystal structure of a purple acid phosphatase containing a dinuclear Fe(III)–Zn(II) active site. Science 268:1489–1492
23. Kissinger CR, Parge HE, Knighton DR et al (1995) Crystal structures of human calcineurin and the human FKBP12–FK506-calcineurin complex. Nature 378:641–644
24. Griffith JP, Kim JL, Kim EE et al (1995) X-ray structure of calcineurin inhibited by the immunophilin-immunosuppressant FKBP12–FK506 complex. Cell 82:507–522
25. Goldberg J, Hsien-bin H, Young-guen K et al (1995) Three-dimensional structure of the catalytic subunit of protein serine/threonine phosphatase-1. Nature 376:745–753
26. Egloff MP, Cohen PTW, Reinemer P, Barford D (1995) Crystal structure of the catalytic subunit of human protein phosphatase 1 and its complex with tungstate. J Mol Biol 254:942–959
27. Fini C, Palmerini CA, Damiani P et al (1990) 5′-nucleotidase from bull seminal plasma, chicken gizzard and snake venom is a zinc metalloprotein. Biochim Biophys Acta 1038:18–22
28. McMillen L, Beacham IR, Burns DM (2003) Cobalt activation of *Escherichia coli* 5′-nucleotidase is due to zinc ion displacement at only one of two metal-ion-binding sites. Biochem J 372:625–630
29. Dvorak HF, Heppel LA (1968) Metallo-enzymes released from *Escherichia coli* by osmotic shock. II. Evidence that 5′-nucleotidase and cyclic phosphodiesterase are zinc metallo-enzymes. J Biol Chem 243:2647–2653
30. Knöfel T, Sträter N (2001) Mechanism of hydrolysis of phosphate esters by the dimetal center of 5′-nucleotidase based on crystal structures. J Mol Biol 309:239–254
31. Stefanovic V, Mandel P, Rosenberg A (1976) Ecto-5′-nucleotidase of intact cultured C6 rat glioma cells. J Biol Chem 251:3900–3905
32. Neu HC (1968) The 5′-nucleotidases (uridine diphosphate sugar hydrolases) of the *Enterobacteriaceae*. Biochemistry 7:3766–3773
33. Grondal EJM, Zimmermann H (1987) Purification, characterization and cellular localization of 5′-nucleotidase from torpedo electric organ. Biochem J 245:805–810
34. Bailyes EM, Soos M, Jackson P et al (1984) The existence and properties of two dimers of rat liver ecto-5′-nucleotidase. Biochem J 221:369–377
35. Buschette-Brambrink S, Gutensohn W (1989) Human placental ecto-5′-nucleotidase: isoforms and chemical cross-linking products of the membrane-bound and isolated enzyme. Biol Chem Hoppe–Seyler 370:67–74
36. Martinez-Martinez A, Munoz-Delgado E, Campoy FJ et al (2000) The ecto-5′-nucleotidase subunits in dimmers are not linked by disulfide bridges but by non-covalent bonds. Biochim Biophys Acta 1478:300–308
37. Fini C, Amoresano A, Andolfo A et al (2000) Mass spectrometry study of ecto-5′-nucleotidase from bull seminal plasma. Eur J Biochem 267:4978–4987
38. Knöfel T, Sträter N (1999) X-ray structure of the *Escherichia coli* periplasmic 5′-nucleotidase containing a dimetal catalytic site. Nat Struct Biol 6:448–451
39. Knöfel T, Sträter N (2001) *E. coli* 5′-Nucleotidase undergoes a hinge-bending domain rotation resembling a ball-and-socket motion. J Mol Biol 309:255–266
40. Schultz-Heienbrok R, Maier T, Sträter N (2005) A large hinge bending domain rotation is necessary for the catalytic function of *Escherichia coli* 5′-nucleotidase. Biochem 44:2244–2252
41. Schultz-Heienbrok R, Maier T, Sträter N (2005) Trapping a 96° domain rotation in two distinct conformations by engineered disulfide bridges. Protein Sci 13:1811–1822